Electronic Supporting Information

for the manuscript entitled

Oxo-bridged Trinuclear and Tetranuclear Manganese Complexes Supported with Nitrogen Donor Ligands: Syntheses, Structures and Properties

Deepak Bansal,[1] Abhishake Mondal,[2] N. Lakshminarasimhan[3] and Rajeev Gupta[1,*]

[1]Department of Chemistry, University of Delhi, Delhi 110 007, India

[2]Solid State and Structural Chemistry Unit, Indian Institute of Science, Bangalore – 560 012, Karnataka, India

[3]Functional Materials Division, CSIR-Central Electrochemical Research Institute (CECRI) Karaikudi – 630 003, Tamil Nadu, India & Academy of Scientific and Innovative Research, CSIR-CECRI Campus, Karaikudi – 630 003, Tamil Nadu, India

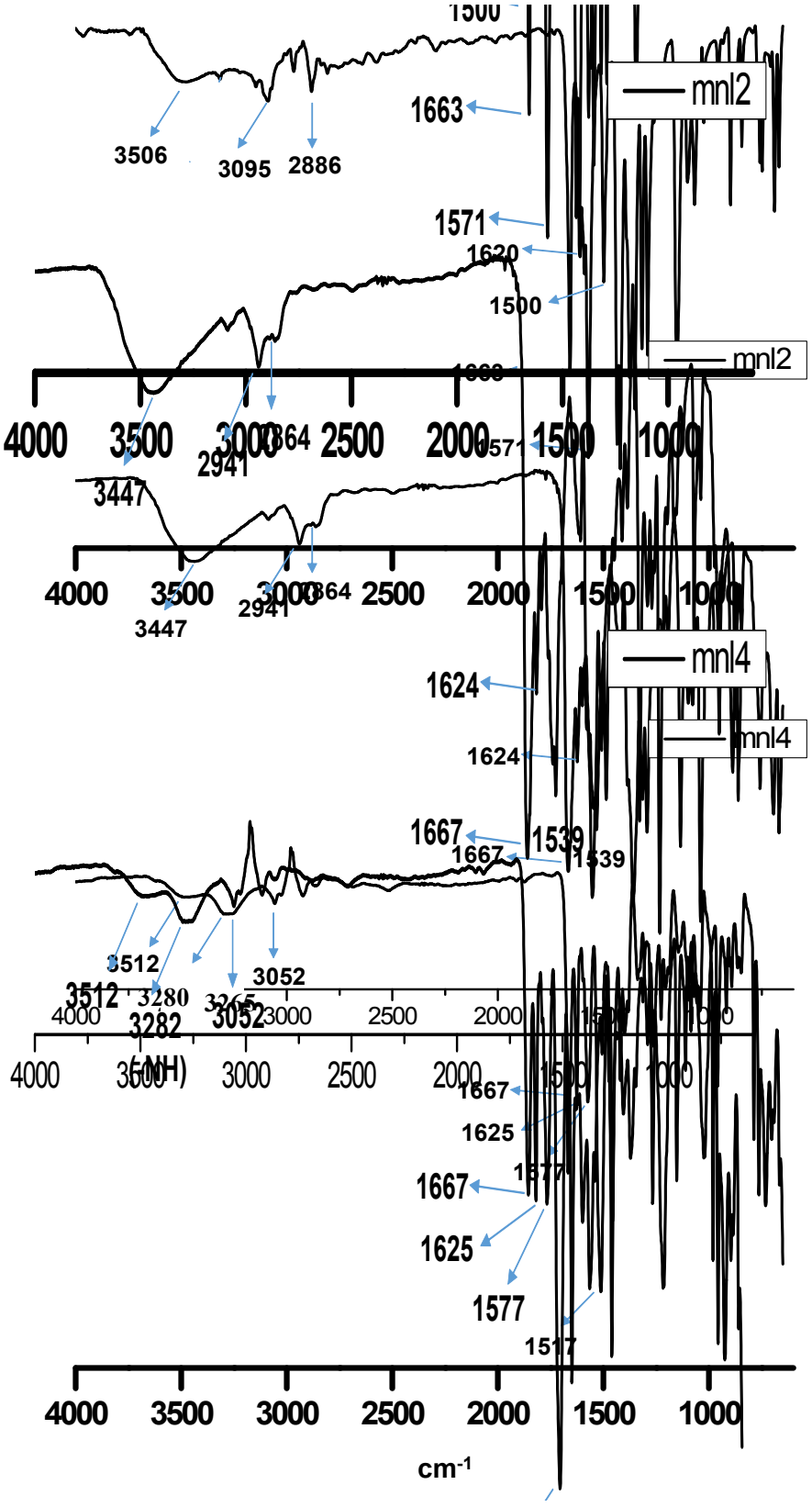

Figure S1. FTIR spectra of complexes **1–3**.

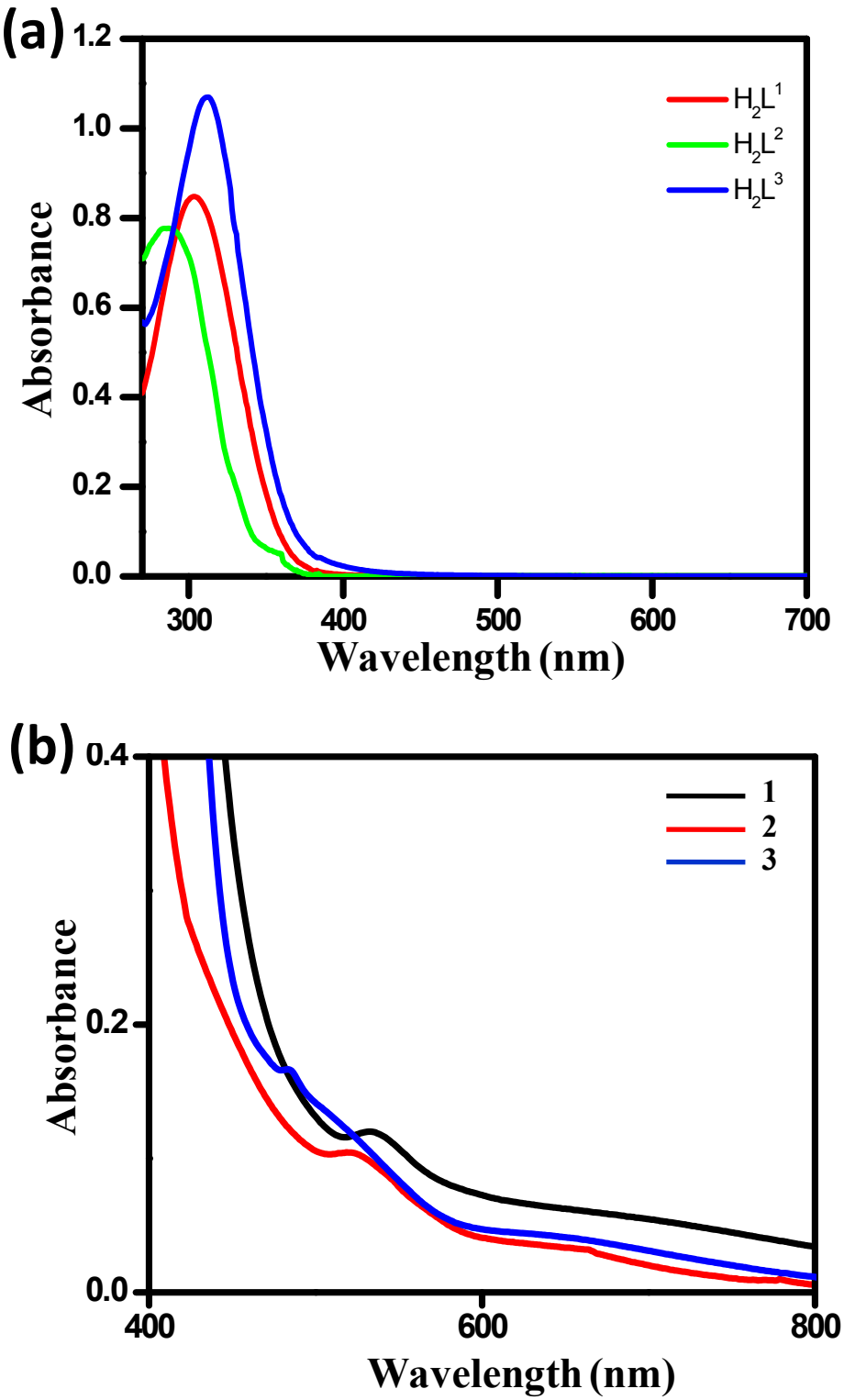

Figure S2. Absorption spectra of (a) ligands H_2L^1-H_2L^3 and (b) complexes **1–3**.

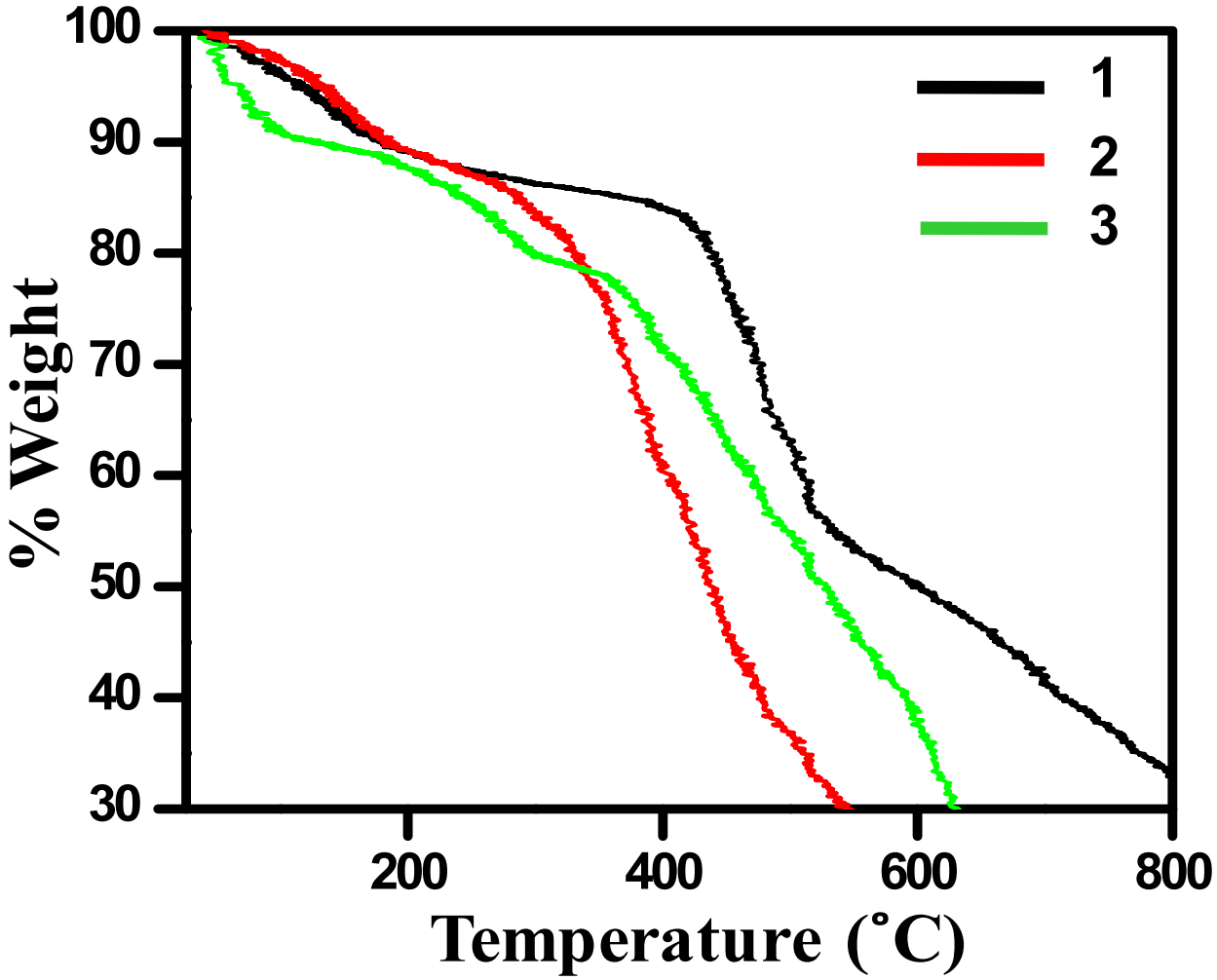

Figure S3. Thermogravimetric analysis (TGA) plots for complexes **1–3**.

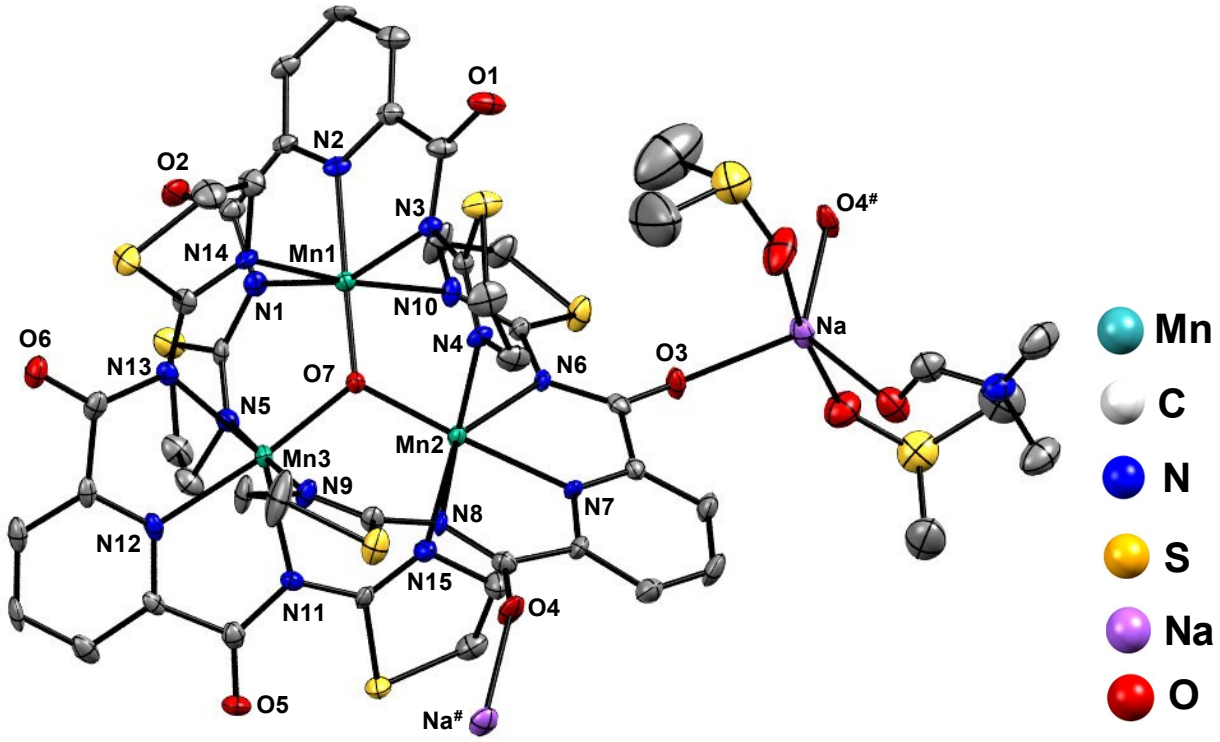

Figure S4. Thermal ellipsoidal representation, drawn at 30% probability level, of complex **2**. Hydrogen atoms and lattice H_2O molecule are omitted for clarity.

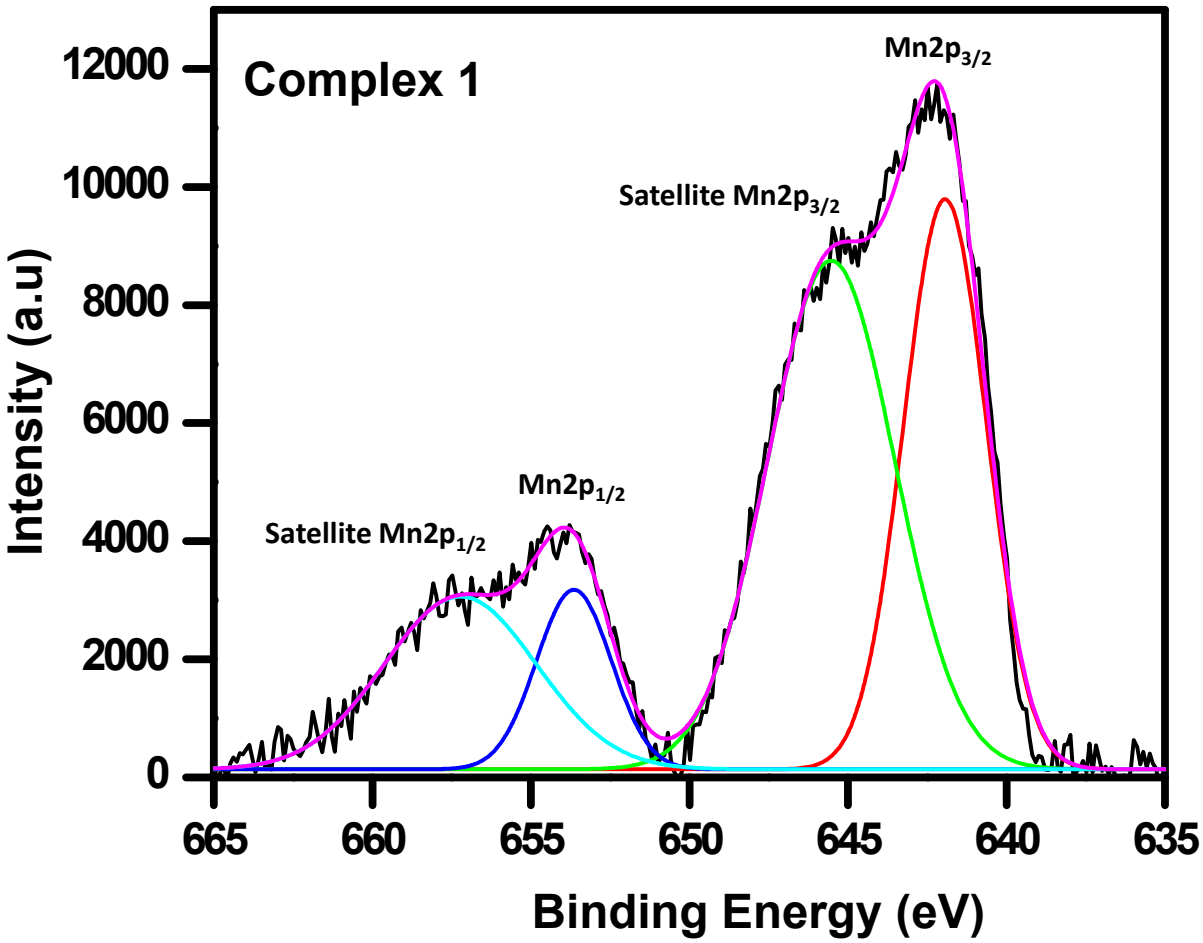

Figure S5. De-convoluted Mn2p XPS spectrum of complex **1**.

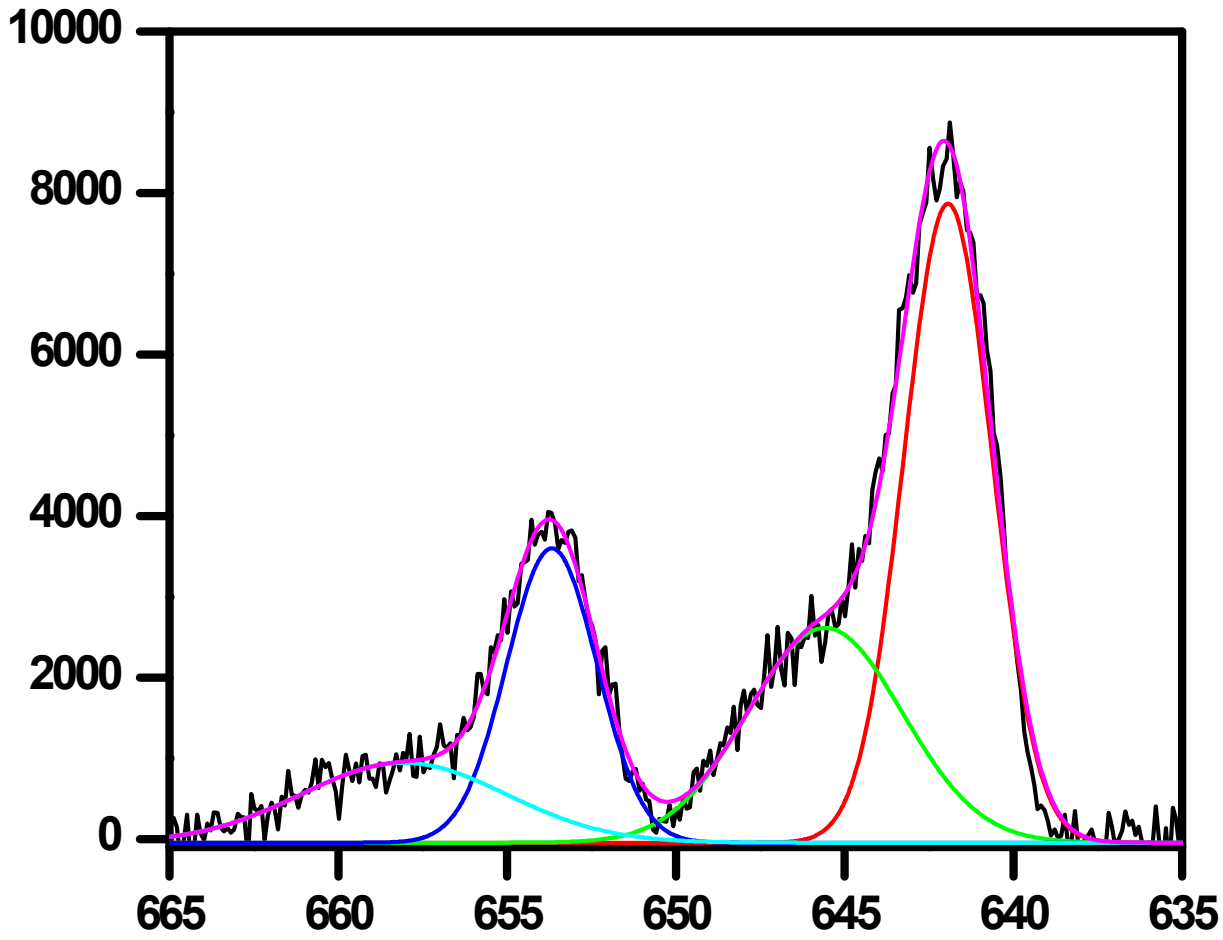

Figure S6. De-convoluted Mn2p XPS spectrum of complex **2**.

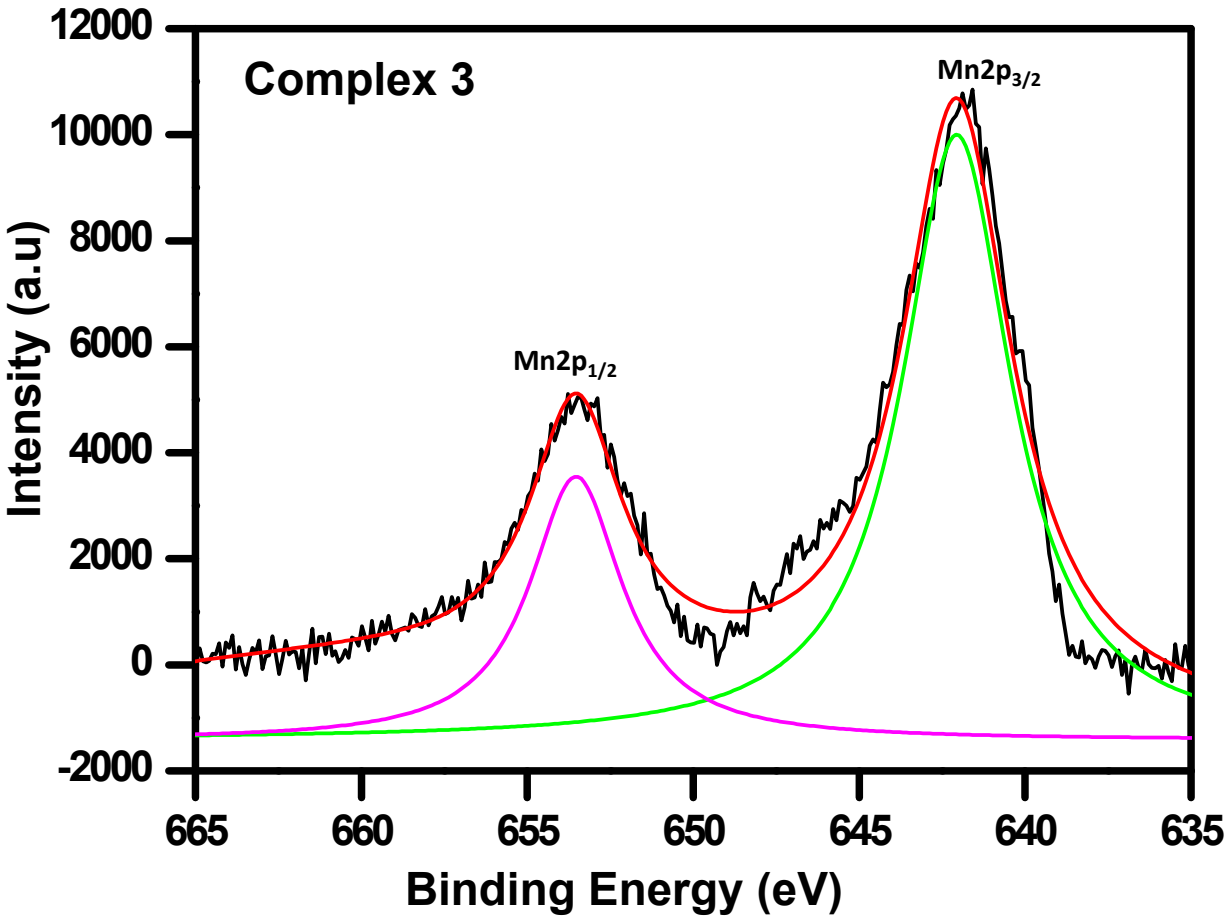

Figure S7. De-convoluted Mn2p XPS spectrum of complex **3**.

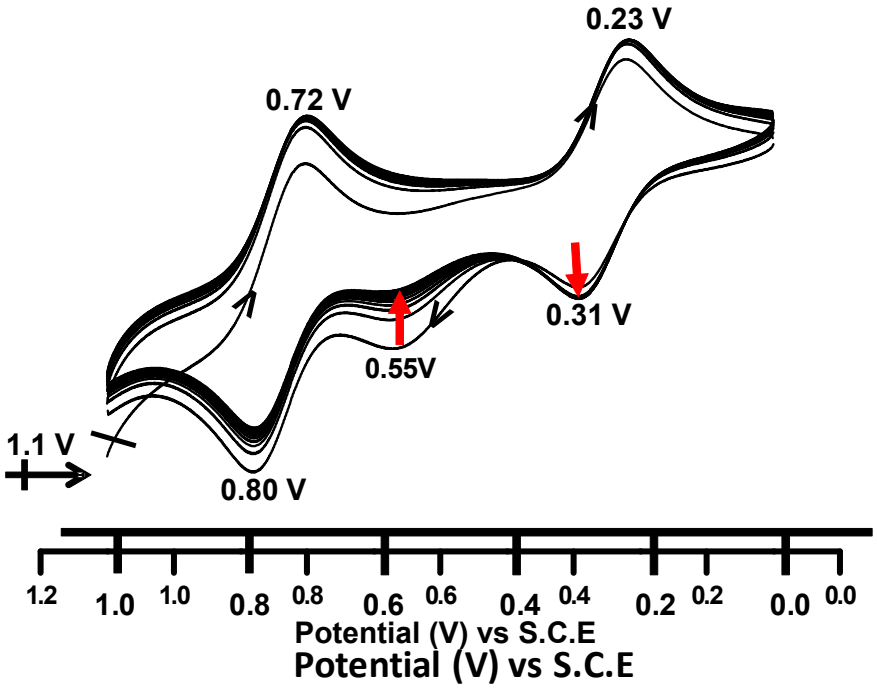

Figure S8. Cyclic voltammetric traces for complex **1** displaying disappearance of an electrochemical response at ca. 0.58 V on multiple scans.

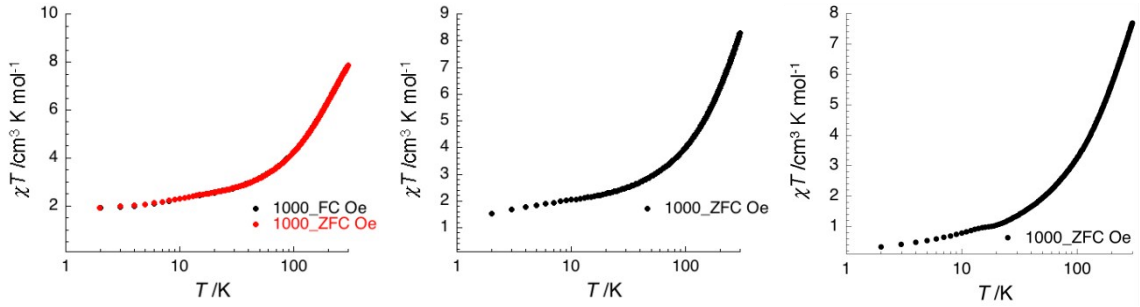

Figure S9. Temperature dependence of χT product (log scale) at 1000 Oe for polycrystalline samples for complexes **1** (left), **2** (middle) and **3** (right).

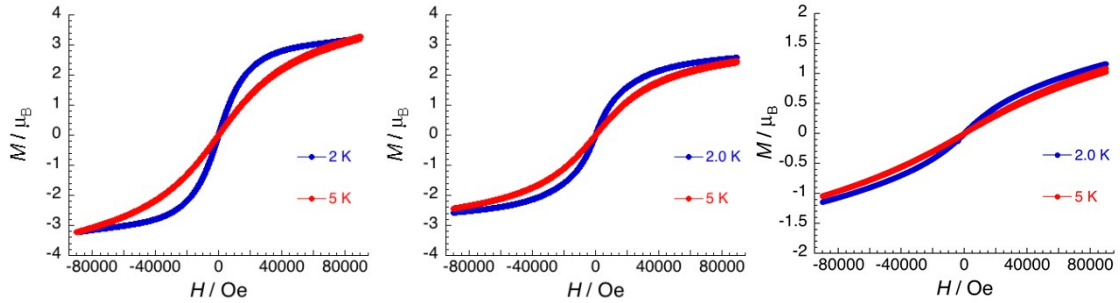

Figure S10. Field dependence of the magnetization as *M vs H* plots for complexes **1** (left), **2** (middle) and **3** (right) at 2 and 5 K, respectively.

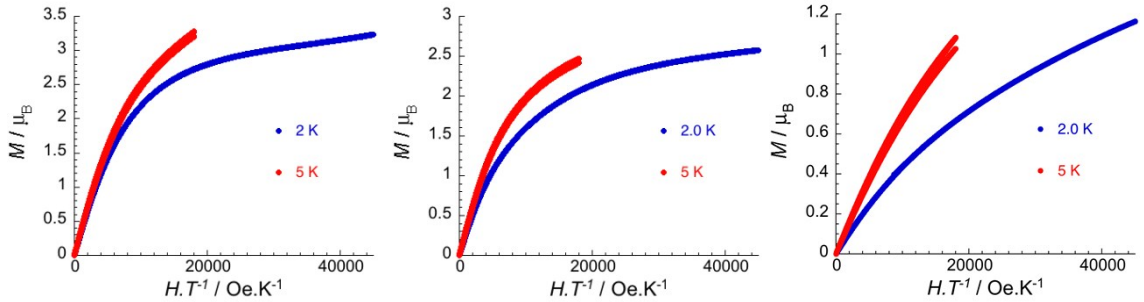

Figure S11. Field dependence of the magnetization as *M vs H/T* plots for complexes **1** (left), **2** (middle) and **3** (right) at 2 and 5 K, respectively.

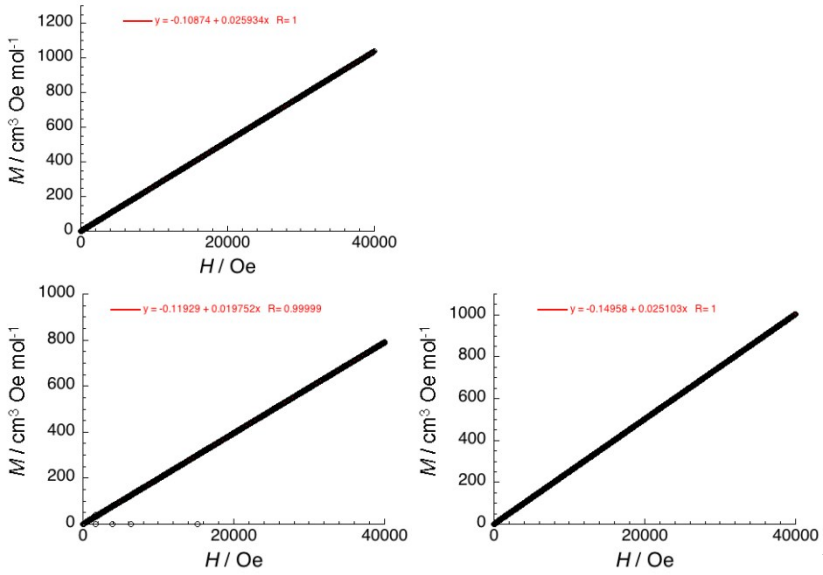

Figure S12. Field dependence of the magnetization for complexes **1** (left), **2** (middle) and **3** (right) collected at 300 K. The red line represents the linear fit to the data.

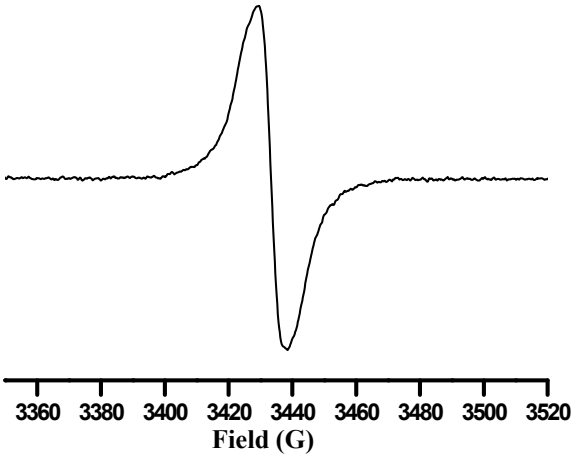

Figure S13. Solid-state EPR spectrum of polycrystalline sample of complex **1** recorded at 77K.

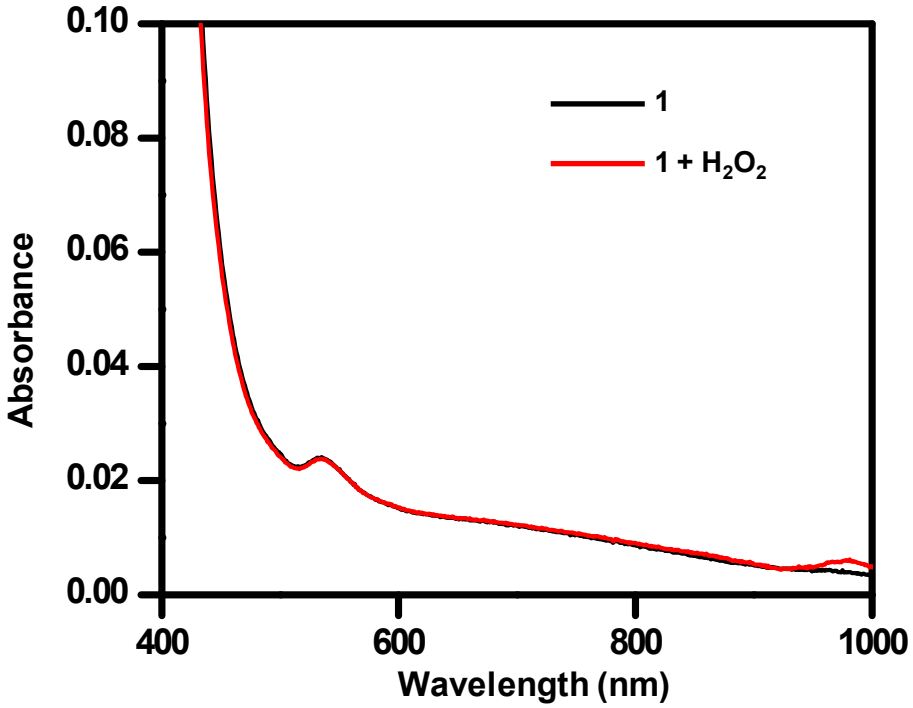

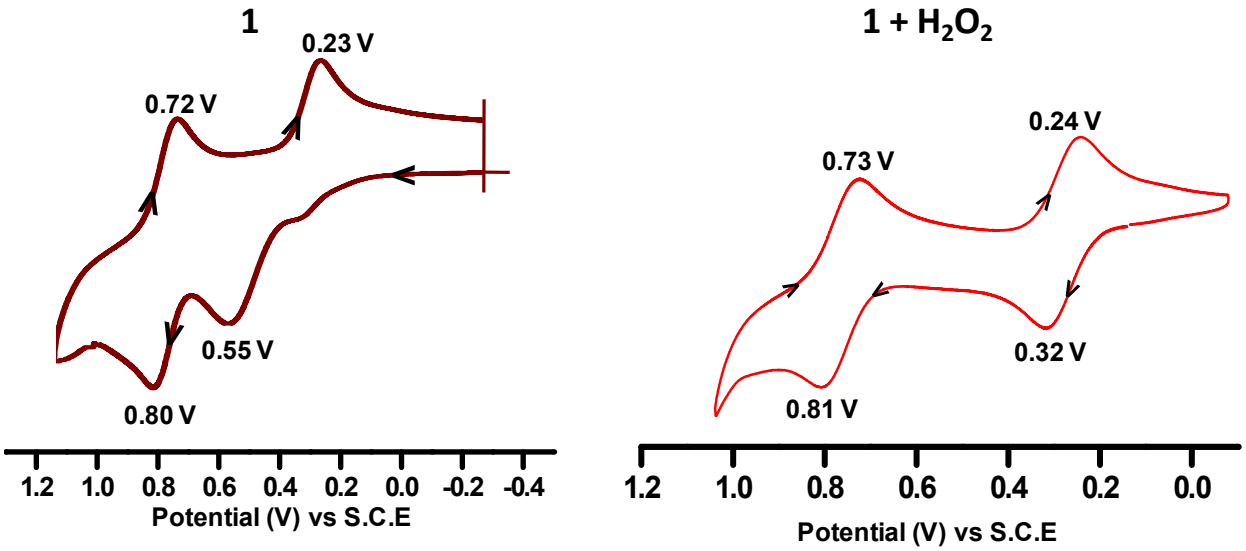

Figure S14. Changes in the absorption spectra (top) and cyclic voltammograms (bottom) of complex **1** on addition of 150 equiv. of H_2O_2.

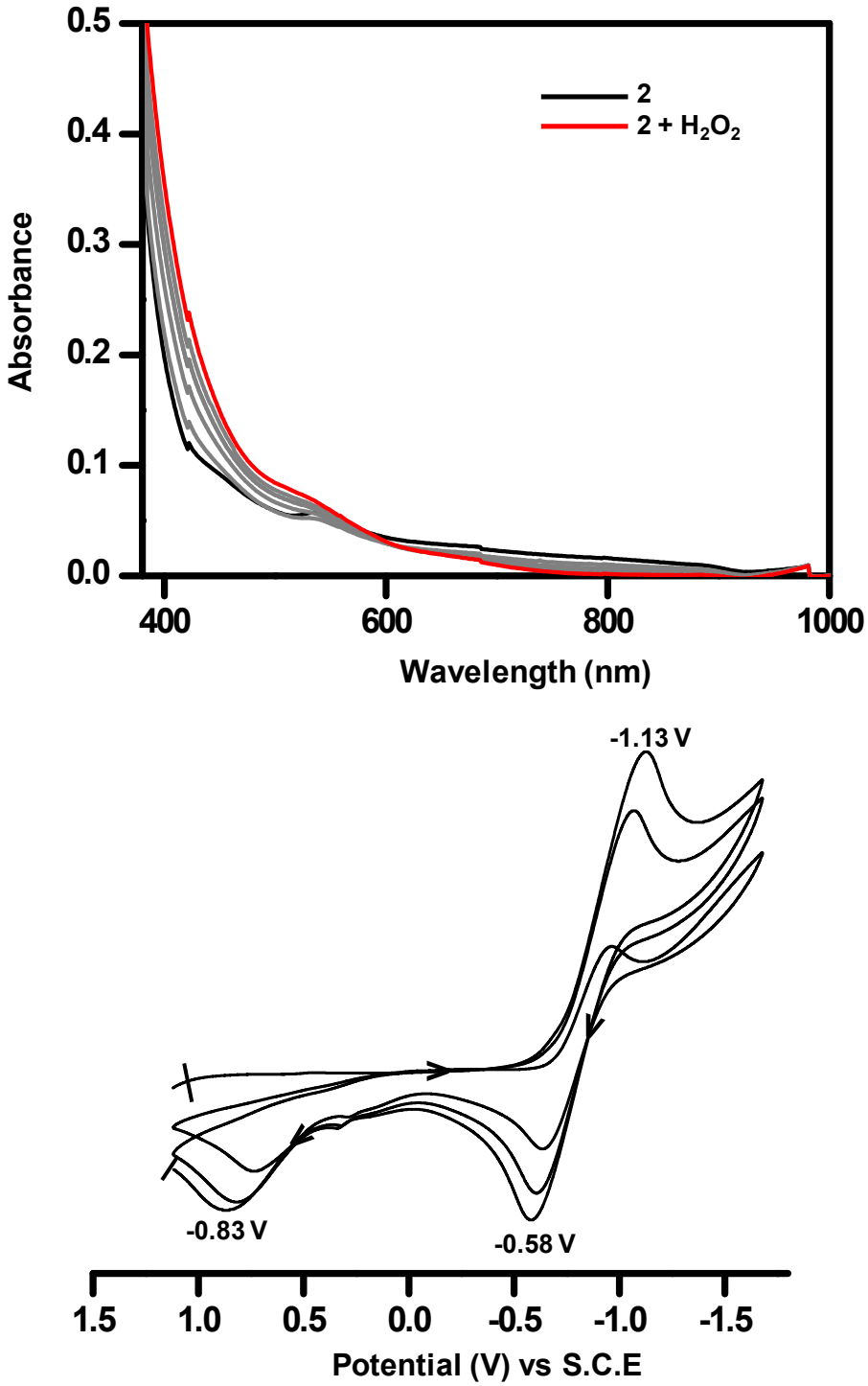

Figure S15. Changes in the absorption spectra (top) and cyclic voltammograms (bottom) of complex **2** on addition of 150 equiv. of H_2O_2.

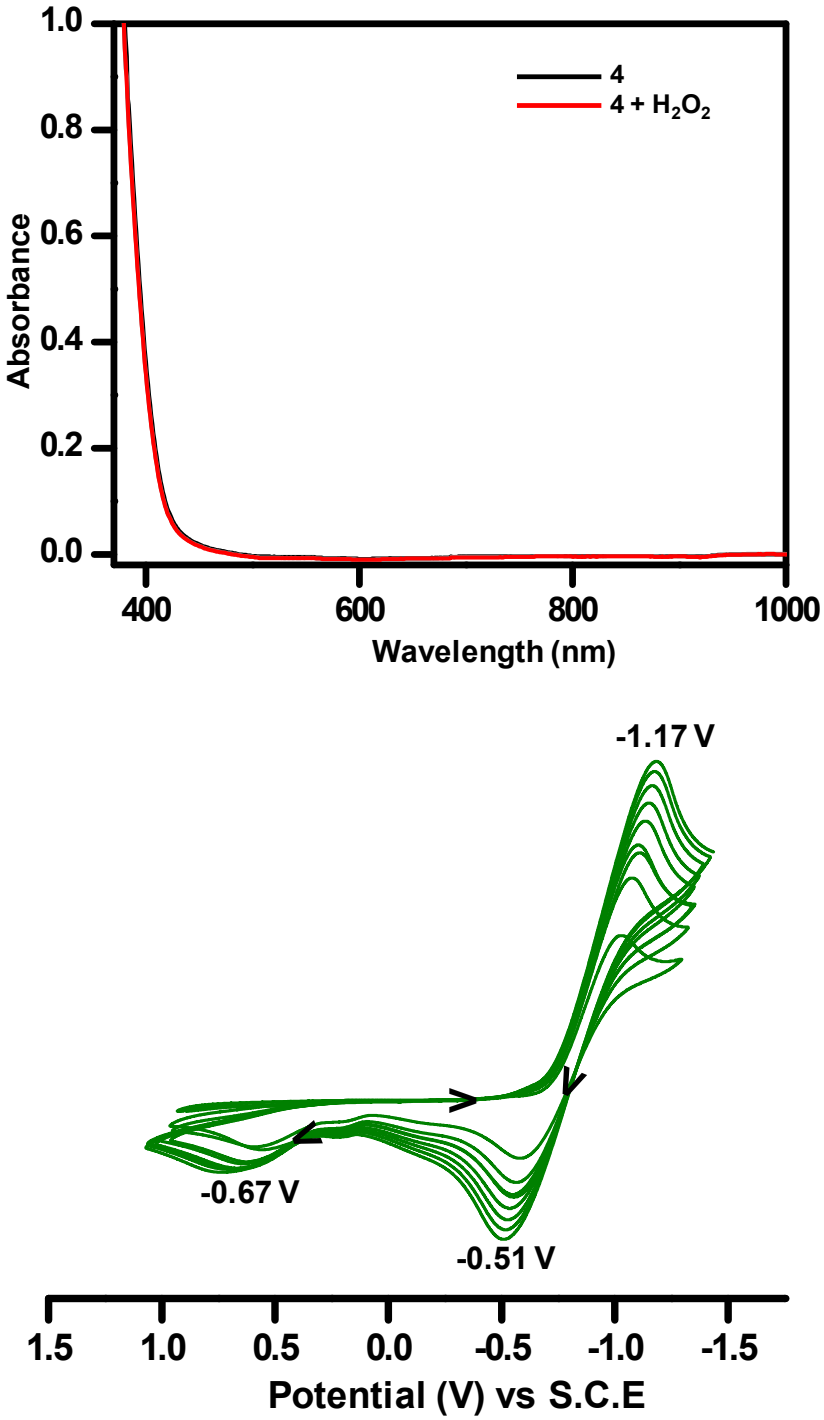

Figure S16. Changes in the absorption spectra (top) and cyclic voltammograms (bottom) of complex **3** on addition of 150 equiv. of H_2O_2.

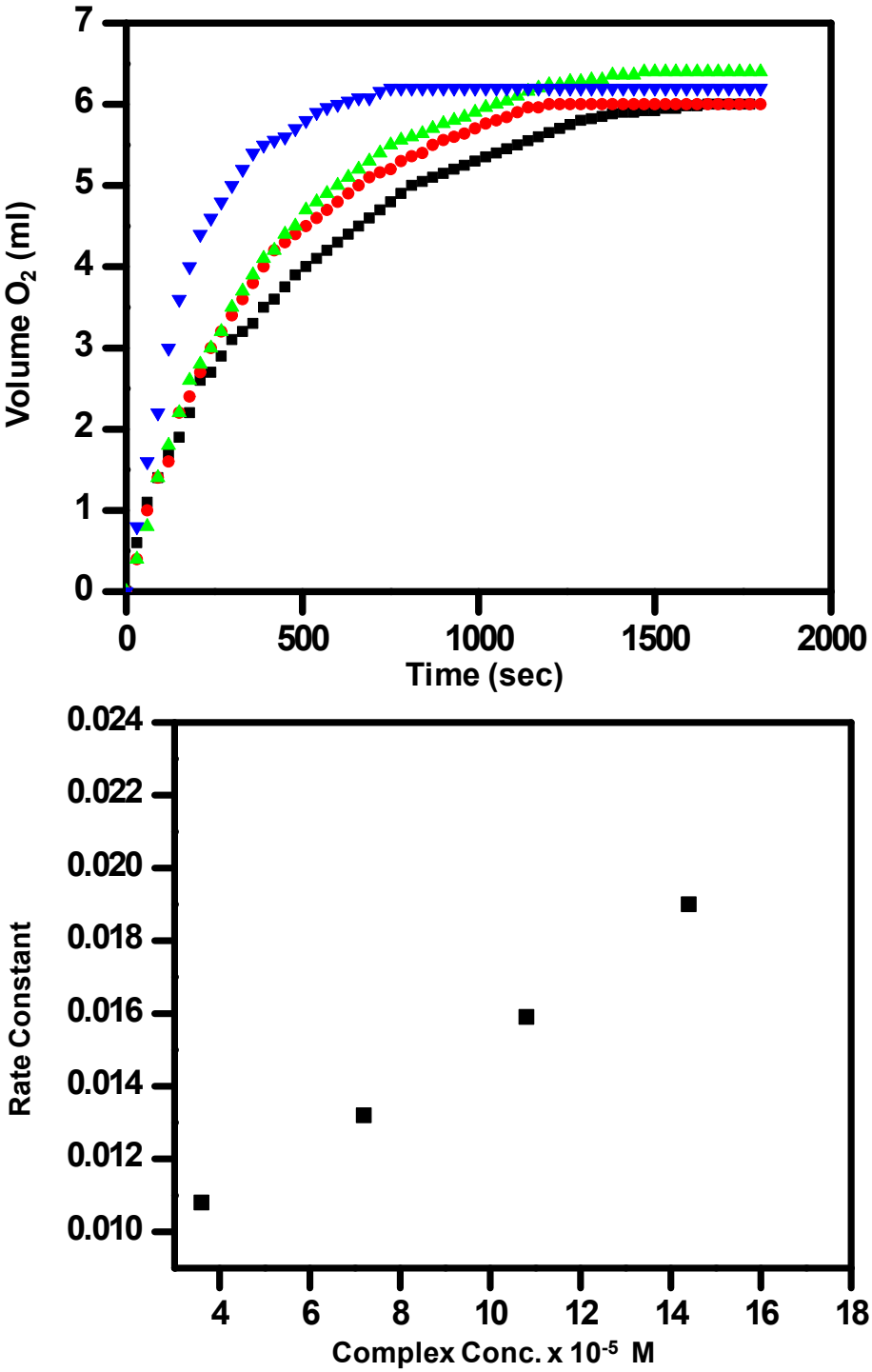

Figure S17. Top: Change in the volume of evolved O_2 with different concentration of complex **2** keeping constant $[H_2O_2]$. Bottom: rate change in O_2 evolution as a function of complex concentration.

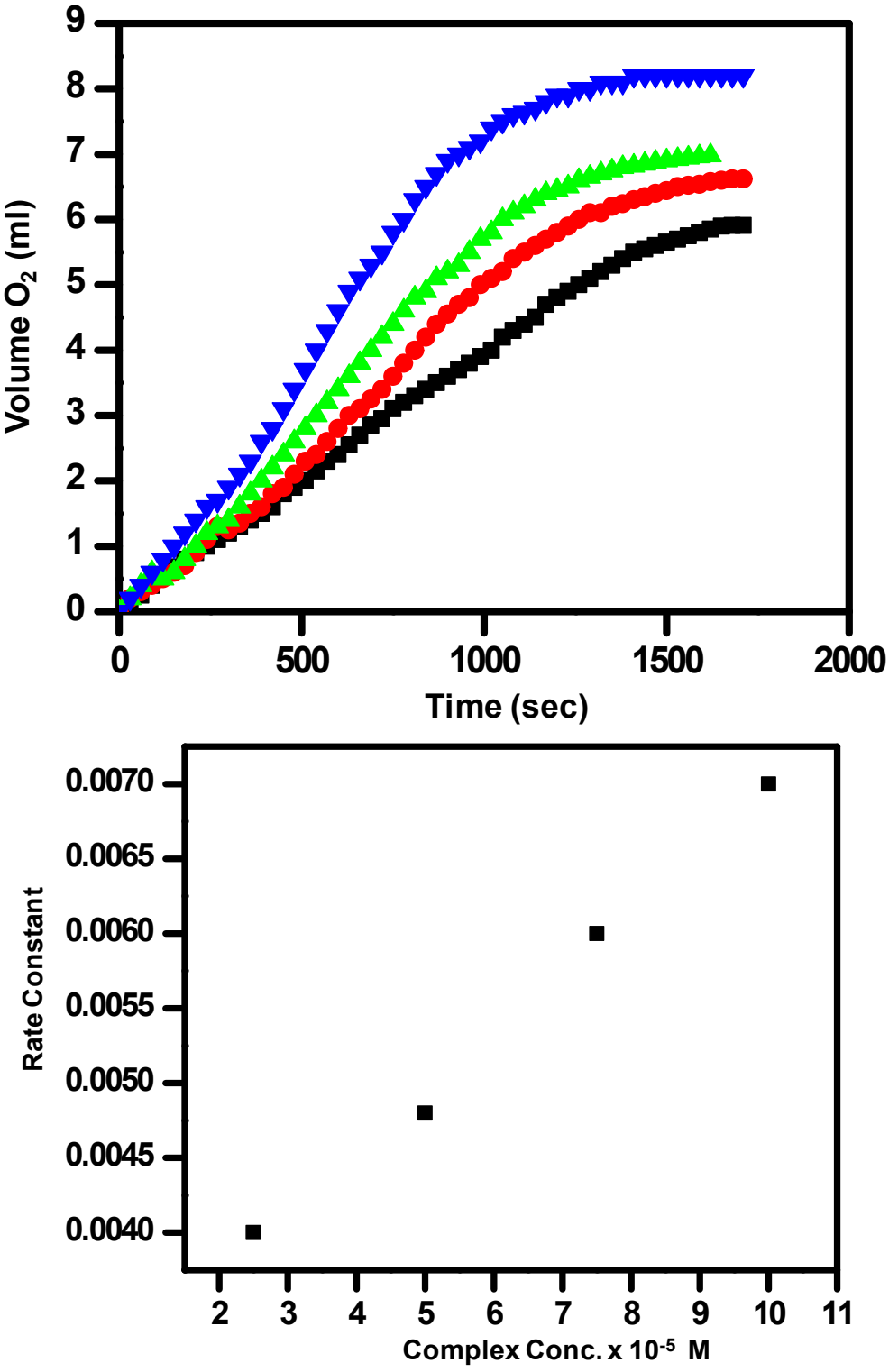

Figure S18. Top: Change in the volume of evolved O_2 with different concentration of complex **3** keeping constant $[H_2O_2]$. Bottom: rate change in O_2 evolution as a function of complex concentration.

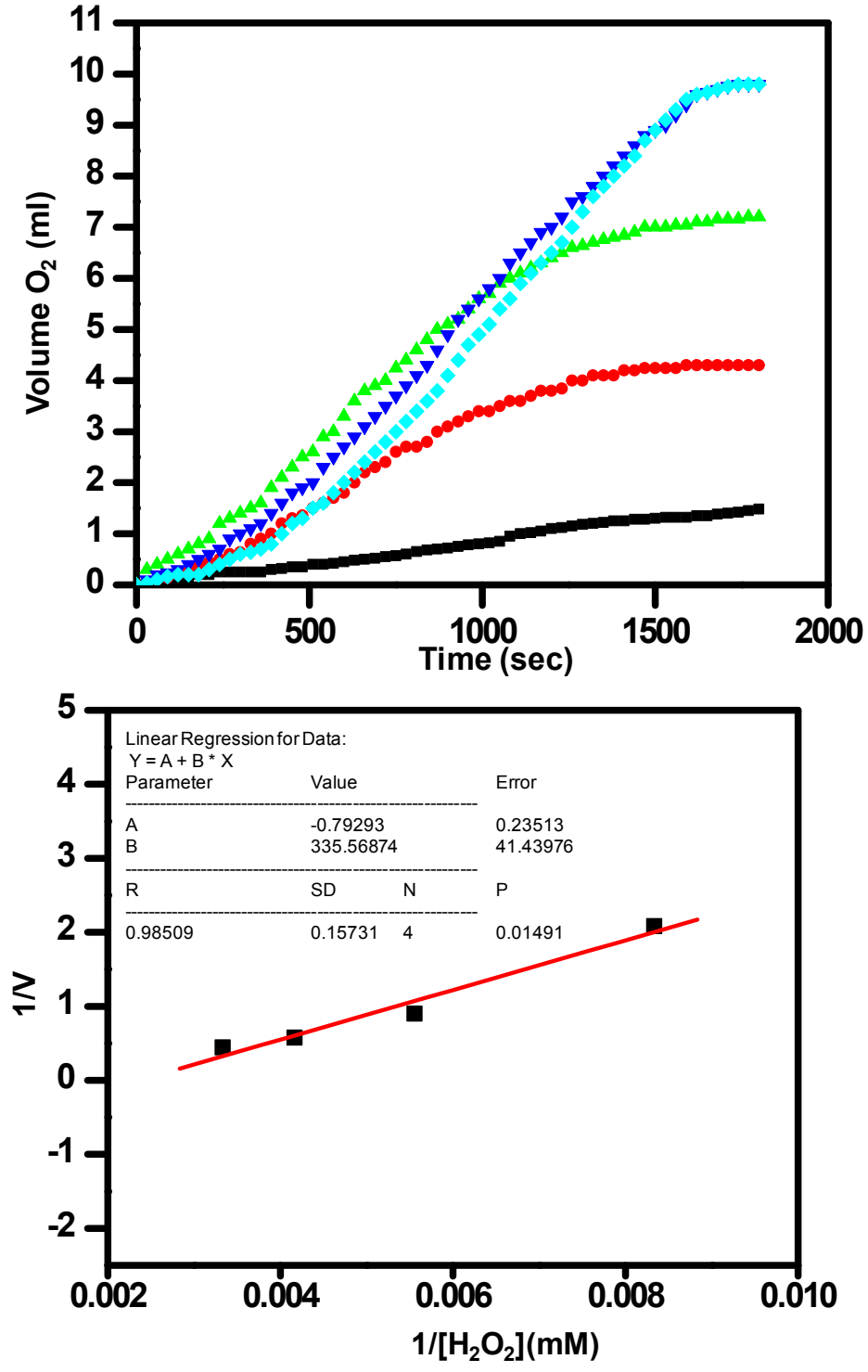

Figure S19. Top: Time-dependent evolution of O_2 after successive additions of H_2O_2 (150-750 equiv.) to a solution of complex **2**. Bottom: Lineweaver–Burk plot between 1/V and 1/[H_2O_2].

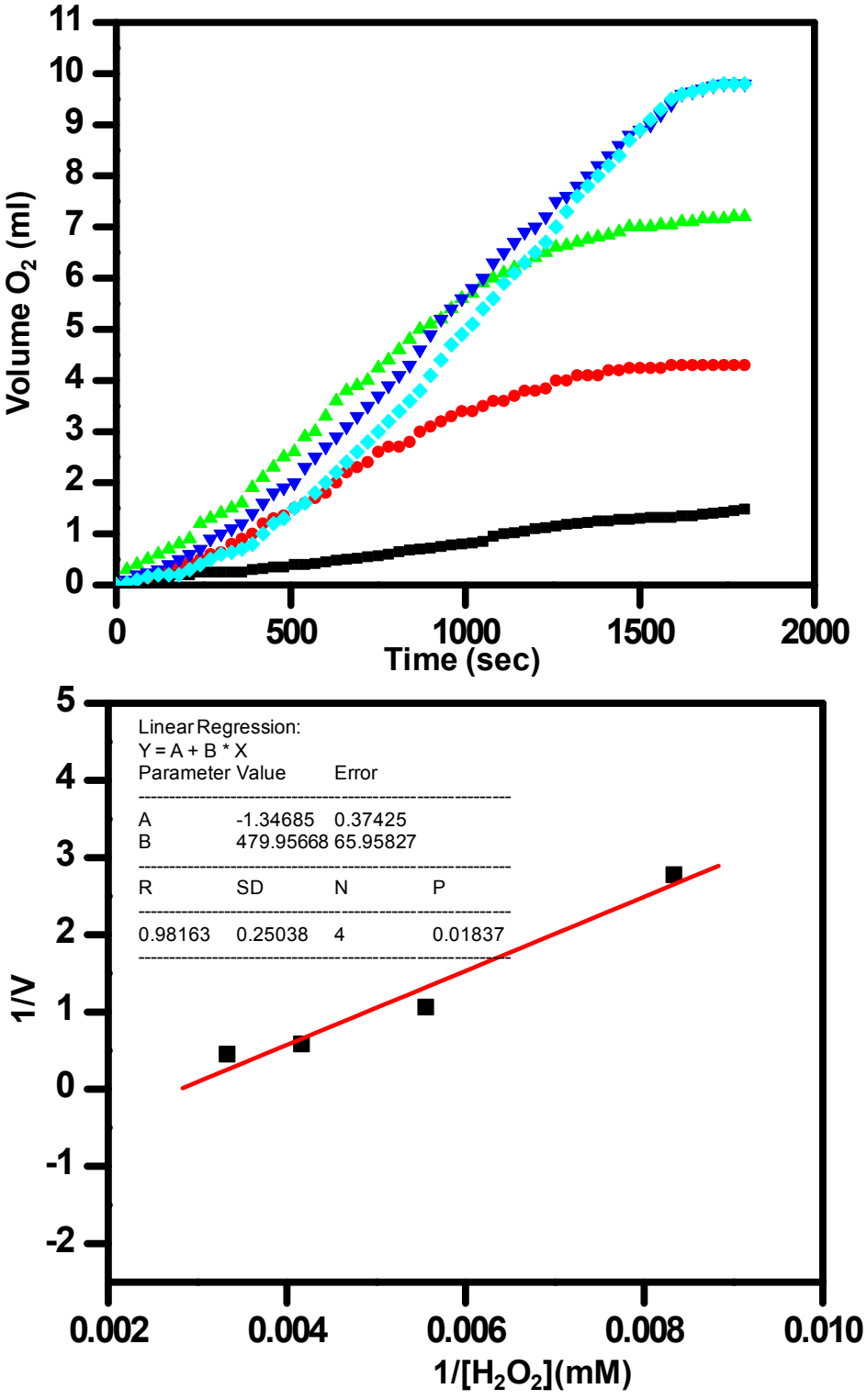

Figure S20. Top: Time-dependent evolution of O_2 after successive additions of H_2O_2 (150-750 equiv.) to a solution of complex **2**. Bottom: Lineweaver–Burk plot between 1/V and 1/[H_2O_2].

Table S1. Crystallographic data collection and structure refinement parameters for complexes **1–3**.

	1	**2**	**3**
Empirical formula	$C_{39}H_{21}Mn_3N_{15}O_7S_6$	$C_{48}H_{58}Mn_3N_{16}NaO_{11}S_9$	$C_{76}H_{71}Mn_4N_{25}O_{12}$
formula mass	1168.89	1511.45	1746.33
T [K]	293(2)	293(2)	293(2)
Crystal system	Triclinic	Orthorhombic	Monoclinic
Space group	*P*-1	*Pbcn*	$P2_1/c$
a [Å]	9.3373(5)	34.750 (2)	13.0764(2)
b [Å]	14.7042(7)	17.5751 (7)	25.6016(5)
c [Å]	24.1731(12)	20.5572 (11)	24.1881(4)
α [°]	95.157(4)	90	90
β [°]	91.831(4)	90	93.0681(18)
γ [°]	100.293(4)	90	90
V [Å^3]	3248.4(3)	12555.0 (11)	8086.0 (3)
Z	2	8	4
d [g cm^{-3}]	1.195	1.599	1.434
μ [mm^{-1}]	0.815	0.970	0.687
F(000)	1174	6208	3592
Final *R* indices [I>2σ(I)][a]	R_1 = 0.0981 wR_2 = 0.2081	R_1 = 0.1043 wR_2 = 0.2010	R_1 = 0.0710 wR_2 = 0.1846
R indices (all data)	R_1 = 0.1622 wR_2 = 0.2357	R_1 = 0.1535 wR_2 = 0.2236	R_1 = 0.1148 wR_2 = 0.2089
GOF (F^2)	1.023	1.094	1.030
CCDC	1900796	1900797	1900798

[a] $R_1 = \Sigma||F_o|-|F_c||/\Sigma|F_o|$; $wR = \{[\Sigma(|F_o|^2|F_c|^2)^2]\}^{1/2}$

Table S2. Selected bond distances (Å) and bond angles (°) for complexes **1**–**3**.

Atoms	**1**	Atoms	**2**	Atoms	**3**
Mn(1)-O(7)	2.001(5)	Mn(1)-O(7)	1.744(5)	N(1)-Mn(1)	2.273(4)
Mn(1)-N(2)	2.167(5)	Mn(1)-N(2)	1.999(7)	N(2)-Mn(1)	2.196(4)
Mn(1)-N(3)	2.200(6)	Mn(1)-N(3)	2.124(7)	N(3)-Mn(1)	2.251(4)
Mn(1)-N(1)	2.252(6)	Mn(1)-N(1)	2.126(7)	N(4)-Mn(4)	2.188(4)
Mn(1)-N(10)	2.348(6)	Mn(1)-N(14)	2.357(7)	N(5)-Mn(3)	2.176(4)
Mn(1)-N(15)	2.460(7)	Mn(1)-N(10)	2.408(7)	N(6)-Mn(2)	2.259(4)
Mn(2)-O(7)	1.909(6)	Mn(2)-O(7)	1.963(5)	N(7)-Mn(2)	2.159(4)
Mn(2)-N(7)	2.131(6)	Mn(2)-N(7)	2.167(6)	N(8)-Mn(2)	2.307(4)
Mn(2)-N(8)	2.216(6)	Mn(2)-N(8)	2.243(7)	N(9)-Mn(4)	2.153(4)
Mn(2)-N(6)	2.228(5)	Mn(2)-N(6)	2.272(6)	N(10)-Mn(1)	2.164(4)
Mn(2)-N(4)	2.434(7)	Mn(2)-N(4)	2.370(7)	N(11)-Mn(3)	2.281(4)
Mn(2)-N(14)	2.469(6)	Mn(2)-N(15)	2.429(7)	N(12)-Mn(3)	2.177(4)
Mn(3)-O(7)	1.934(5)	Mn(3)-O(7)	1.978(5)	N(13)-Mn(3)	2.267(4)
Mn(3)-N(12)	2.135(6)	Mn(3)-N(12)	2.184(7)	N(14)-Mn(4)	2.168(4)
Mn(3)-N(13)	2.228(6)	Mn(3)-N(11)	2.244(7)	N(15)-Mn(2)	2.185(4)
Mn(3)-N(11)	2.231(6)	Mn(3)-N(13)	2.277(7)	O(7)-Mn(2)	2.007(3)
Mn(3)-N(9)	2.312(7)	Mn(3)-N(5)	2.352(7)	O(7)-Mn(3)	2.006(3)
-------	-------	Mn(3)-N(9)	2.394(7)	O(7)-Mn(1)	2.009(3)
-------	-------	-------	-------	O(7)-Mn(4)	2.120(3)
-------	-------	-------	-------	O(9)-Mn(4)	2.253(5)
Bond Angles (°)					
O(7)-Mn(1)-N(2)	172.5(2)	O(7)-Mn(1)-N(2)	178.4(3)	O(7)-Mn(1)-N(10)	107.05(15)
O(7)-Mn(1)-N(3)	111.6(2)	O(7)-Mn(1)-N(3)	102.0(3)	O(7)-Mn(1)-N(2)	141.97(15)
N(2)-Mn(1)-N(3)	74.0(2)	N(2)-Mn(1)-N(3)	77.2(3)	N(10)-Mn(1)-N(2)	109.62(16)
O(7)-Mn(1)-N(1)	100.8(2)	O(7)-Mn(1)-N(1)	102.8(3)	O(7)-Mn(1)-N(3)	95.68(14)
N(2)-Mn(1)-N(1)	73.6(2)	N(2)-Mn(1)-N(1)	78.0(3)	N(10)-Mn(1)-N(3)	94.71(16)
N(3)-Mn(1)-N(1)	147.5(2)	N(3)-Mn(1)-N(1)	155.2(3)	N(2)-Mn(1)-N(3)	71.81(15)
O(7)-Mn(1)-N(10)	90.0(2)	O(7)-Mn(1)-N(14)	93.0(2)	O(7)-Mn(1)-N(1)	105.62(14)
N(2)-Mn(1)-N(10)	95.1(2)	N(2)-Mn(1)-N(14)	88.4(3)	N(10)-Mn(1)-N(1)	107.91(16)
N(3)-Mn(1)-N(10)	88.9(2)	N(3)-Mn(1)-N(14)	88.9(2)	N(2)-Mn(1)-N(1)	72.20(15)
N(1)-Mn(1)-N(10)	91.2(2)	N(1)-Mn(1)-N(14)	89.7(2)	N(3)-Mn(1)-N(1)	142.21(16)
O(7)-Mn(1)-N(15)	86.9(2)	O(7)-Mn(1)-N(10)	91.7(2)	O(7)-Mn(2)-N(7)	152.43(15)
N(2)-Mn(1)-N(15)	88.5(2)	N(2)-Mn(1)-N(10)	86.9(3)	O(7)-Mn(2)-N(15)	109.33(15)
N(3)-Mn(1)-N(15)	88.0(2)	N(3)-Mn(1)-N(10)	87.0(2)	N(7)-Mn(2)-N(15)	97.33(16)

N(1)-Mn(1)-N(15)	93.9(2)	N(1)-Mn(1)-N(10)	92.4(2)	O(7)-Mn(2)-N(6)	107.12(14)
N(10)-Mn(1)-N(15)	174.5(2)	N(14)-Mn(1)-N(10)	174.3(2)	N(7)-Mn(2)-N(6)	73.61(15)
O(7)-Mn(2)-N(7)	175.4(3)	O(7)-Mn(2)-N(7)	176.5(2)	N(15)-Mn(2)-N(6)	100.54(16)
O(7)-Mn(2)-N(8)	107.1(2)	O(7)-Mn(2)-N(8)	110.0(2)	O(7)-Mn(2)-N(8)	97.35(14)
N(7)-Mn(2)-N(8)	73.7(2)	N(7)-Mn(2)-N(8)	73.3(2)	N(7)-Mn(2)-N(8)	71.20(16)
O(7)-Mn(2)-N(6)	104.4(2)	O(7)-Mn(2)-N(6)	102.8(2)	N(15)-Mn(2)-N(8)	98.47(16)
N(7)-Mn(2)-N(6)	74.8(2)	N(7)-Mn(2)-N(6)	73.8(2)	N(6)-Mn(2)-N(8)	141.70(15)
N(8)-Mn(2)-N(6)	148.4(2)	N(8)-Mn(2)-N(6)	147.2(2)	O(7)-Mn(3)-N(5)	108.08(14)
O(7)-Mn(2)-N(4)	93.2(2)	O(7)-Mn(2)-N(4)	88.1(2)	O(7)-Mn(3)-N(12)	145.83(15)
N(7)-Mn(2)-N(4)	91.2(2)	N(7)-Mn(2)-N(4)	91.3(2)	N(5)-Mn(3)-N(12)	105.97(15)
N(8)-Mn(2)-N(4)	95.3(2)	N(8)-Mn(2)-N(4)	87.1(2)	O(7)-Mn(3)-N(13)	97.77(14)
N(6)-Mn(2)-N(4)	84.6(2)	N(6)-Mn(2)-N(4)	94.2(2)	N(5)-Mn(3)-N(13)	102.45(16)
O(7)-Mn(2)-N(14)	87.1(3)	O(7)-Mn(2)-N(15)	93.0(2)	N(12)-Mn(3)-N(13)	71.91(15)
N(7)-Mn(2)-N(14)	88.5(2)	N(7)-Mn(2)-N(15)	88.1(2)	O(7)-Mn(3)-N(11)	104.72(14)
N(8)-Mn(2)-N(14)	83.6(2)	N(8)-Mn(2)-N(15)	83.7(2)	N(5)-Mn(3)-N(11)	99.01(16)
N(6)-Mn(2)-N(14)	96.4(2)	N(6)-Mn(2)-N(15)	94.6(2)	N(12)-Mn(3)-N(11)	72.39(15)
N(4)-Mn(2)-N(14)	178.9(2)	N(4)-Mn(2)-N(15)	170.6(2)	N(13)-Mn(3)-N(11)	142.15(15)
O(7)-Mn(3)-N(12)	164.2(3)	O(7)-Mn(3)-N(12)	173.6(2)	O(7)-Mn(4)-N(9)	91.19(14)
O(7)-Mn(3)-N(13)	104.4(3)	O(7)-Mn(3)-N(11)	112.5(2)	O(7)-Mn(4)-N(14)	92.38(14)
N(12)-Mn(3)-N(13)	73.3(2)	N(12)-Mn(3)-N(11)	73.2(3)	N(9)-Mn(4)-N(14)	112.66(16)
O(7)-Mn(3)-N(11)	105.9(2)	O(7)-Mn(3)-N(13)	101.7(2)	O(7)-Mn(4)-N(4)	90.21(15)
N(12)-Mn(3)-N(11)	74.0(2)	N(12)-Mn(3)-N(13)	72.5(3)	N(9)-Mn(4)-N(4)	122.08(16)
N(13)-Mn(3)-N(11)	147.0(2)	N(11)-Mn(3)-N(13)	145.7(2)	N(14)-Mn(4)-N(4)	125.12(16)
O(7)-Mn(3)-N(9)	94.9(3)	O(7)-Mn(3)-N(5)	86.9(2)	O(7)-Mn(4)-O(9)	174.53(16)
N(12)-Mn(3)-N(9)	100.8(2)	N(12)-Mn(3)-N(5)	90.3(2)	N(9)-Mn(4)-O(9)	92.69(18)
N(13)-Mn(3)-N(9)	93.6(2)	N(11)-Mn(3)-N(5)	89.8(2)	N(14)-Mn(4)-O(9)	89.69(18)
N(11)-Mn(3)-N(9)	96.4(2)	N(13)-Mn(3)-N(5)	90.4(2)	N(4)-Mn(4)-O(9)	84.46(18)
-------	-------	O(7)-Mn(3)-N(9)	91.3(2)	-------	-------
-------	-------	N(12)-Mn(3)-N(9)	91.6(2)	-------	-------
-------	-------	N(11)-Mn(3)-N(9)	89.2(2)	-------	-------
-------	-------	N(13)-Mn(3)-N(9)	91.7(2)	-------	-------
-------	-------	N(5)-Mn(3)-N(9)	177.5(2)	-------	-------
Mn(2)-O(7)-Mn(3)	118.9(3)	Mn(1)-O(7)-Mn(2)	124.8(3)	Mn(2)-O(7)-Mn(3)	110.79(15)
Mn(2)-O(7)-Mn(1)	116.3(3)	Mn(1)-O(7)-Mn(3)	123.8(3)	Mn(2)-O(7)-Mn(1)	113.98(15)
Mn(3)-O(7)-Mn(1)	122.8(3)	Mn(2)-O(7)-Mn(3)	111.4(3)	Mn(3)-O(7)-Mn(1)	111.20(15)
-------	-------	-------	-------	Mn(2)-O(7)-Mn(4)	104.96(14)

-------	-------	-------	-------	Mn(3)-O(7)-Mn(4)	109.05(15)
-------	-------	-------	-------	Mn(1)-O(7)-Mn(4)	106.48(15)